Refining Gluon Distributions in Nucleons via Lattice QCD

Lattice 2024, Liverpool

Lorenzo Maio
On behalf of the *HadStruc Collaboration*

Aix Marseille Univ, Université de Toulon, CNRS, CPT, Marseille, France

July 30, 2024

Introduction

The computation of the gluon PDFs is needed for the precise computation of a number of observables, as the cross-sections for the jet production and the Higgs boson production measured at LHC, or the J/ψ photo production measuread at Jefferson Lab.

Global analyses of data from deep inelastic scattering and related processes allow to access information on the PDFs and future colliders are expected to improve the precision on the determination of gluon PDFs.

Current efforts are devoted to increase the precision on the gluon distribution $xg(x)$ and in the understanding of the suppression in $0.1 < x < 0.4$ when ATLAS and CMS data on the jet production are included.

Introudction

Computing PDFs on the lattice is important from a theoretical point of view, as it allows to get insights on the non-perturbative properties of the QCD from first principles.

Several strategies have been proposed for the extraction of the x-dependent hadron structure from lattice data:

- path integral formulation of the DIS hadronic tensor;
- OPE;
- lattice cross sections;
- quasi-PDF;
- **pseudo-PDF**.

Introduction

Our goal is to refine predictions on the Gluon Distribution in Nucleons already presented in *HadStruc, Phys. Rev. D* ***104*** *(2021) no.9, 094516 [2107.08960]*, extend it to more lattice spacings and pion masses, in order to attain a continuum prediction at the physical point.

Data production and analysis is still ongoing, and this talk will be focused on a new strategy to extract more precise estimations of the relevant matrix elements, that we are currently testing.

In the context of the pseudo-PDF approach, we ccompute the pseudo-ITD $\mathfrak{M}(\nu, z^2)$, whose Fourier transform returns the pseudo-PDF $\mathcal{P}(x, z^2)$, that in turn is the Lorentz invariant generalization of the PDF we are interested in.

We apply the *reduced* pseudo-ITD approach, where the multiplicative UV renormalization factors in $\mathfrak{M}(\nu, z^2)$ are canceled by computing a ratio of the relevant matrix elements

$$\mathfrak{M}(\nu, z^2) = \frac{\mathcal{M}(p, z)}{\mathcal{M}(0, z)} \Big/ \frac{\mathcal{M}(p, 0)}{\mathcal{M}(0, 0)}, \tag{1}$$

making the reduced pseudo-ITD becomes an RGI quantity. Then, we compute the gluon PDF through the short distance factorization.

The matrix element appearing in the RHS of Eq. (1) can be computed as

$$\mathcal{M} = M_{ti;it} + M_{ji;ij}, \tag{2}$$

where

$$M_{\mu\nu;\nu\mu}(z,p) = 2\,\langle p|\,G_{\mu\nu}(z)\,W[z,0]\,G_{\nu\mu}(0)\,W[0,z]|p\rangle\,, \tag{3}$$

$W[z,0]$ is the straight Wilson line of length z connecting the gluon fields $G_{\mu\nu}(0)$ and $G_{\mu\nu}(z)$ and p^μ is the nucleon momentum.

Such expectation values can be calculated on the lattice. As the gluonic currents are not connected to the nucleon state by quark propagators, we compute separately the two-point function and the gluon operator and then we combine them to get the relevant three points function.

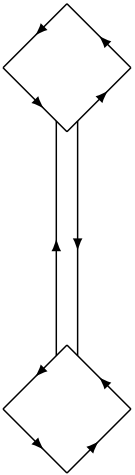

The gluonic currents can be computed as

$$O_{\mu\nu;\nu\mu}(z) = P_{\mu\nu}(z)\, U_3(z) P_{\nu\mu}(0)\, U_3(z)^\dagger, \tag{4}$$

where P is the "open" plaquette operator, and U_3 the Wilson lines connecting (and closing) the plaquettes. To reduce statistical fluctuations, each plaquette is the average of the four possible realizations obtainable by changing μ and ν signs.

Taking into account the change of sign due to the Wick rotation, the total gluonic current becomes

$$O_g(z) = P_{ji}(z)\, U_3(z) P_{ij}(0)\, U_3(z)^\dagger - P_{ti}(z)\, U_3(z) P_{it}(0)\, U_3(z)^\dagger. \tag{5}$$

Lattice operators

To compute the nucleon two-points correlators we apply distillation, an approximation to the gauge-covariant Jacobi-smearing kernel. Such method allows to compute the computational-demanding propagators (called *perambulators* in this context) on the gauge fields once, and then to use them on a large basis of interpolators. This is suitable to perform a (summed) GEVP analysis.

Moreover, distillation allows to perform momentum smearing on both source and sink interpolating operator, in contrast to the most customary methods. Thus, we are able to impose momentum projection on all the three time slices of our three-point function.

Last but not least, the low-lying levels of the nucleon can be captured with a relatively small number of distillation eigenvectors, thus lowering the cost of the computation.

Lattice operators

The interpolating operators are chosen in order to have the largest overlap with the ground state and the lowest excited states.

Spatial momentum	Interpolators
$\vec{p} = \vec{0}$	$N\,^2S_S\,\frac{1}{2}^+,\ N\,^2S_M\,\frac{1}{2}^+,\ N\,^4D_M\,\frac{1}{2}^+,$ $N\,^2P_A\,\frac{1}{2}^+,\ N\,^4P^*_M\,\frac{1}{2}^+,\ N\,^2P^*_M\,\frac{1}{2}^+$
$\vec{p} \neq \vec{0}$	$N\,^2P_M\,\frac{1}{2}^-,\ N\,^2P_M\,\frac{3}{2}^-,\ N\,^4P_M\,\frac{1}{2}^-,$ $N\,^4P_M\,\frac{3}{2}^-,\ N\,^4P_M\,\frac{5}{2}^-,\ N\,^2S_S\,\frac{1}{2}^+,$ $N\,^2S_M\,\frac{1}{2}^+,\ N\,^2P^*_M\,\frac{1}{2}^+,\ N\,^4P^*_M\,\frac{1}{2}^+$

In the table, a spectroscopic notation is adopted to indicate the operator: $N^{2S+1}L_\pi J^P$, where S is the Dirac spin, L the orbital angular momentum; π is the permutation simmetry, J the total angular momentum and P the parity.

Finally, the three point function is computed as

$$C^{ij}_{3pt}(t, t_g) = (C^{ij}_{2pt}(t) - < C^{ij}_{2pt}(t) >)(O_g - < O_g(t_g) >), \tag{6}$$

where

$$C_{2pt}{}^{ij}(t) = < O^i(0)\ O^j(t) >, \tag{7}$$

$O^i(t)$ being the i^{th} interpolator.

To extract the matrix elements from C_{3pt} we imlement the sGEVP method, which consists of a combination of the summation method and the standard GEVP, and requires to compute the summed three-point function

$$C^s_{3pt}(t) = \sum_{t_g=1}^{t-1} C_{3pt}(t, t_g). \tag{8}$$

The generalized eigenvalue problem of the two-point correlator matrix is stated as follows

$$C_{2pt}(t)\mathbf{u}_n(t,t_0) = \lambda_n(t,t_0)\, C_{2pt}(t_0)\mathbf{u}_n(t,t_0) \tag{9}$$

where n denotes the energy level (we aim to solve the system for N energy levels where N is the number of interpolators), $\mathbf{u}_n(t,t_0)$ is a generalized eigenvector, $\lambda_n(t,t_0)$ the principal correlator. Solving the problem, means rotating the two-points correlator in the basis spanned by the generalized eigenvectors, leading to a better identification of the low lying states contributions. Then, the energy can be obtained by fitting the principal correlator

$$\lambda_n(t,t_0) = (1-A_n)e^{-E_n(t-t0)} + A_n e^{-E'_n(t-t_0)}. \tag{10}$$

When the fit is dominated by the leading exponential $A_n \ll 1$, and $E'_n > E_n$.

The summed GEVP generalizes the GEVP, allowing to compute the interesting matrix elment

$$\mathcal{M}_{nn}^{eff,s}(t,t_0) = -\partial_t \frac{(\mathbf{u}_n(t,t_0), [C_{3pt}^s(t)\lambda_n^{-1}(t,t_0) - C_{3pt}^s(t_0)]\mathbf{u}_n(t,t_0))}{(\mathbf{u}_n(t,t_0), C_{2pt}(t_0)\mathbf{u}_n(t,t_0))}, \qquad (11)$$

which consists in rotating the three point correlator in the same basis where the two-point one is diagonal, which results in the suppression of the excited states contributions to the three-point correlator as well.

Our aim is to improve the GEVP results by projecting the two point function in the operator subspace with the largest overlap with the ground state.

The overlap factors can be easily computed, as they are related to the eigenvectors by

$$Z_i^n = \langle n| O_i^\dagger |0\rangle = \sqrt{2m_n} e^{m_n t_0/2} u_n^{j\,*} C^{ji}(t_0), \tag{12}$$

and comparing them allows to determine what are the operators that contribute the most to the ground state isolation.

Then, one can build the projector on the subspace spanned by the most important operators using the eigenvectors.

$$P = \sum_{i \in \{\mathcal{O}\}} \mathbf{e}^i \otimes \mathbf{e}^i, \quad \text{where} \quad \mathbf{e}^{\mathrm{i}} = \mathbf{u}^{\mathrm{i}} - \sum_{\mathrm{k}=0}^{\mathrm{i}-1} (\mathbf{e}^{\mathrm{k}}, \mathbf{u}^{\mathrm{i}})\ \mathbf{e}^{\mathrm{k}}, \tag{13}$$

and i runs on the most important operators. The Gram–Schmidt algorithm is used because the u_n^i rows are not orthonormal.

The projection

Then, our procedure consists in performing again a GEVP analysis but using the projected correlator, thus solving the system of equation

$$C^P_{2pt}(t)\mathbf{u}_n(t,t_0) = \lambda_n(t,t_0)\, C^P_{2pt}(t_0)\mathbf{u}_n(t,t_0), \tag{14}$$

where

$$C^P_{2pt}(t) = PC_{2pt}(t). \tag{15}$$

is an $M \times M$ matrix, where M is the number of selected operators on which we performed the projection. Then, we construct the three-point correlator using $C^P_{2pt}(t)$, and evaluate the effective matrix element through the sGEVP as shown above.

We expect this method to improve the ground state identification, sacrificing precision on the excited states, which, however, are not interesting in this context.

Lattice details

We performed an exploratory study on an $N_f = 2 + 1$ ensemble with stout-link smeared clover Wilson fermions (with isotropic ρ=0.125) and a tree-level improved Symanzik gauge action, with lattice spacing $a \simeq 0.094$ fm and Pion mass $M_\pi \simeq 358$ MeV, and spatial and temporal size, respectively 32 a and 64 a, generated by the JLab/W&M collaboration.

We used 227 configurations gauge separated by 10 HMC trajectories and 64 temporal sources, and studied the effect of the projection on two different spatial momentum classes: $(0, 0, 0)$, and $(0, 0, p_z)$.

Momentum (0,0,0)

Best operators:

$$N^2 S_S \tfrac{1}{2}^+, \quad N^2 S_M \tfrac{1}{2}^+, \quad N^2 P^*_M \tfrac{1}{2}^+.$$

	Standard				Projected			
t_0	χ/d.o.f.	aE_0	A_0	aE'_0	χ/d.o.f.	aE_0	A_0	aE'_0
4	1.52	0.5311(13)	0.046(6)	1.117(61)	3.28	0.5308(19)	0.090(14)	0.911(61)
5	1.30	0.5310(13)	0.026(5)	1.117(61)	3.09	0.5301(21)	0.066(17)	0.862(71)
6	1.04	0.5310(14)	0.014(4)	1.117(61)	3.35	0.5324(10)	0.026(3)	1.063(24)
7	1.08	0.5325(11)	0.004(1)	1.117(61)	2.92	0.5322(11)	0.016(2)	1.057(23)

Table: Principal correlator fit results for the static two-points correlator.

$$\lambda_n(t, t_0) = (1 - A_n) e^{-E_n(t-t0)} + A_n e^{-E'_n(t-t_0)}. \tag{16}$$

Results for the GEVP

Momentum (0,0,0)

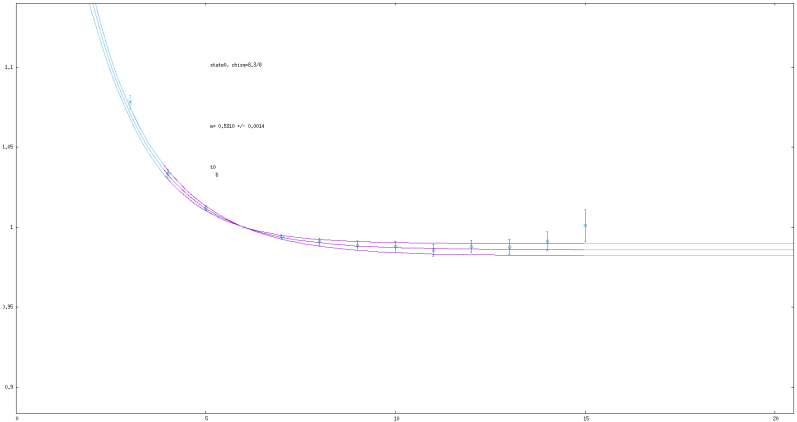

Figure: Standard GEVP results at $t_0 = 6$

Results for the GEVP

Momentum (0,0,0)

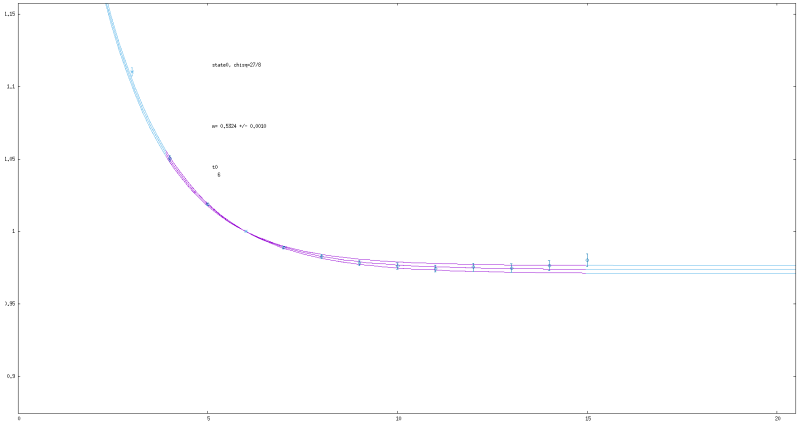

Figure: Projected-GEVP result $t_0 = 6$

Momentum (0,0,1)

Best operators:

$$N^2 S_S \tfrac{1}{2}^+, \quad N^2 P^*_M \tfrac{1}{2}^+, \quad N^4 P^*_M \tfrac{1}{2}^+.$$

	Standard				Projected			
t_0	χ/d.o.f.	aE_0	A_0	aE'_0	χ/d.o.f.	aE_0	A_0	aE'_0
4	2.81	0.5674(16)	0.061(8)	1.071(53)	2.24	0.5669(13)	0.052(5)	1.079(26)
5	2.86	0.5676(15)	0.037(7)	1.080(53)	2.23	0.5668(13)	0.032(4)	1.079(26)
6	2.74	0.5682(14)	0.020(5)	1.105(54)	2.21	0.5668(13)	0.019(3)	1.079(26)
7	2.32	0.5685(14)	0.011(3)	1.121(52)	2.17	0.5667(13)	0.012(2)	1.079(26)

Table: Principal correlator fit results for the two-points correlator with momentum $p = (0, 0, 1)$.

$$\lambda_n(t, t_0) = (1 - A_n) e^{-E_n(t-t0)} + A_n e^{-E'_n(t-t_0)}. \tag{16}$$

Momentum (0,0,1)

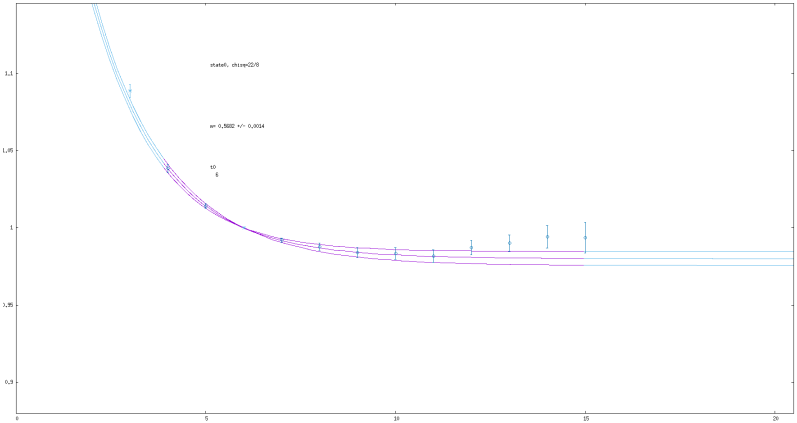

Figure: Standard GEVP results at $t_0 = 6$

Momentum (0,0,1)

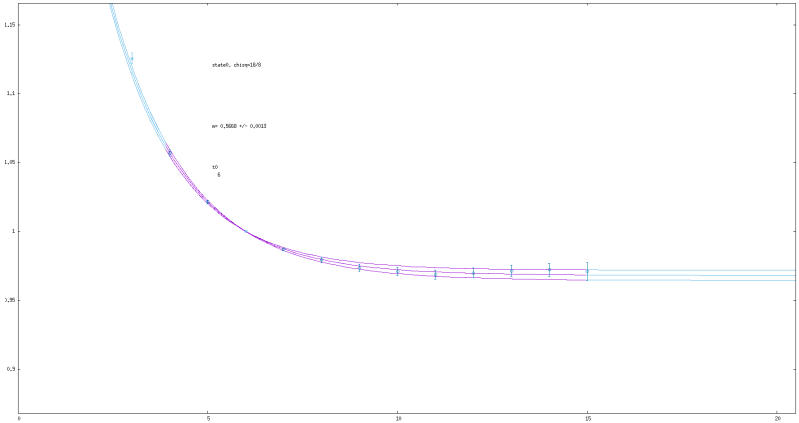

Figure: Projected-GEVP result $t_0 = 6$

Momentum (0,0,2)

Best operators:

$$N^2 S_S \tfrac{1}{2}^+, \quad N^2 P^*_M \tfrac{1}{2}^+, \quad N^4 P^*_M \tfrac{1}{2}^+.$$

	Standard				Projected			
t_0	χ/d.o.f.	aE_0	A_0	aE'_0	χ/d.o.f.	aE_0	A_0	aE'_0
4	0.89	0.6585(28)	0.084(15)	1.153(70)	1.65	0.6584(25)	0.132(13)	1.136(36)
5	0.89	0.6587(29)	0.051(13)	1.162(74)	1.65	0.6585(25)	0.086(11)	1.137(36)
6	0.58	0.6589(28)	0.030(10)	1.174(74)	1.65	0.6585(25)	0.055(9)	1.137(36)
7	0.41	0.6576(30)	0.021(8)	1.151(72)	1.67	0.6585(25)	0.035(7)	1.138(36)

Table: Principal correlator fit results for the two-points correlator with momentum $p = (0, 0, 1)$.

$$\lambda_n(t, t_0) = (1 - A_n) e^{-E_n(t-t0)} + A_n e^{-E'_n(t-t_0)}. \tag{16}$$

Momentum (0,0,2)

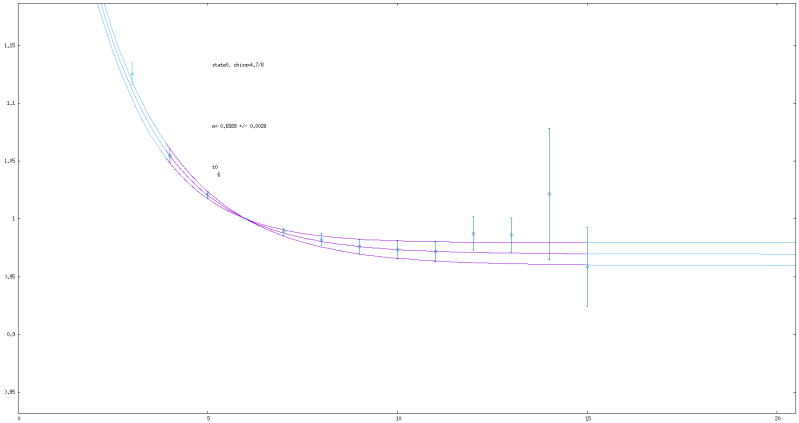

Figure: Standard GEVP results at $t_0 = 6$

Momentum (0,0,2)

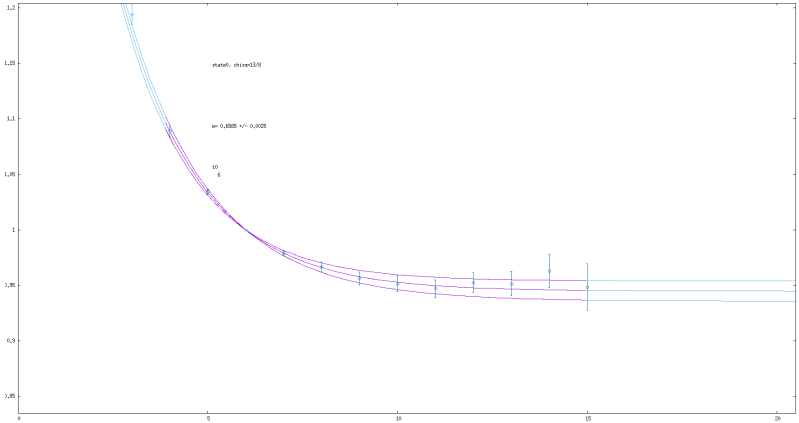

Figure: Projected-GEVP result $t_0 = 6$

Conclusions

For the explored value of lattice spacing and pion Mass, the improvement on the GEVP fits due to the projection on the most relevant operator subspace, if present at all, is marginal.

However, it is not possible to exclude that such strategies could provide an improvement moving toward the physical point and the continuum limit, where excited states are closer to the lowest lying ones, and a better suppression of their contribution would be more relevant.